RSC Mechanochemistry

ROYAL SOCIETY OF CHEMISTRY

COMMUNICATION

View Article Online
View Journal

Cite this: DOI: 10.1039/d5mr00104h

Received 19th August 2025
Accepted 24th November 2025

DOI: 10.1039/d5mr00104h

rsc.li/RSCMechanochem

Biasing mechanistically distinct reaction pathways by mechanochemistry

Hao Luo,† Zhongye Huang,† Yongning Lai,† Yongjie Jiang, Taoyong Wang and KaKing Yan *

Due to the solvent-free nature of the mechanochemical approach, it offers an opportunity to drive reactions with different selectivities from those under conventional solution-based conditions. Nevertheless, literature examples of pathway switching remain scarce. Herein, we report an unusual example where ball-milling offers three distinct pathways leading to three different products. By simply adjusting the amount of liquid additive, arene C–H functionalization can be biased between bromination and oxidation *via* either radical ($Br^{\bullet}$) or ionic (Br^{+}) intermediates, respectively.

In recent years, mechanochemistry has made a comeback in chemical synthesis due to the increased interest in developing greener and more sustainable methods to perform chemical transformations.[1] However, most reported examples emphasize the rate-enhancement aspect of mechanochemical approaches, while their unique role in controlling selectivity,[2] distinct from conventional thermal reactions, has received less attention. For example, Ito reported that mono-arylation is favored over di-arylation for unbiased dibromoarenes by palladium catalysis under ball-milling conditions.[3] Browne described that liquid assisted grinding (LAG) can kinetically bias C–H mono-fluorination over difluorination.[4] Likewise, Mack showed that LAG with various polar solvents lead to different outcomes of Pd-catalyzed alkyne–alkyne coupling reactions.[5] Furthermore, Friščić and co-workers reported that the isolation of elusive aryl *N*-thiocarbamoylbenzotriazole intermediates, which are unobservable by solvent-phase methods, becomes possible under mechanochemical conditions.[6]

Electrophilic bromination is an important industrial reaction for introducing bromine atoms in arenes,[7] as the installed C–Br groups enable subsequent selective functionalizations.[8–10] Traditionally, bromination reactions using either elemental bromine or mild organic bromination agents are predominantly performed under solution-based conditions. Recent advances have demonstrated the feasibility of electrophilic bromination under ball-milling conditions.[11] For example, Mal[11b] and Banerjee[11l] independently showed that bromination proceeded with a broad range of arenes with ball-milling. Hernández presented a mass production protocol using extrusion techniques.[11e]

Although arene bromination has been realized by both solution-based and mechanochemical approaches, most studies have focused on synthetic applications, leaving questions regarding reaction mechanisms and selectivity control largely unaddressed. Understanding the fundamental mechanistic differences between these approaches is critically important, yet it has been largely neglected. This knowledge gap exists because the divergent reactivity observed in mechanochemistry, in our opinion, is difficult to rationally anticipate or design.

Our group is particularly interested in uncovering the insights that explain how these two approaches can drive divergent reactivity from the same starting materials. Consequently, understanding the chemical origin of this unpredictable behavior is paramount for the rational design of divergent synthesis, representing a significant, uncharted area in chemical synthesis. We recently showed a divergent reaction pattern in the reaction of periodic acid and polycyclic aromatic hydrocarbons (PAHs) between ball-milling and solution-based approaches.[12] Specifically, solvent-free mechanochemistry afforded quinones *via* C–H oxidation, whereas the solution-based approach favored a C–H iodination pathway.

During a literature search, we encountered a report by Natarajan,[13] in which the reaction of 9-anthracenecarboxaldehyde (**1a**) with *N*-bromosuccinimide (**2**) in a DMF/H_2O mixture preferentially yielded quinone oxidation products instead of the anticipated C–H bromination product. Motivated to develop chemical processes with reduced carbon footprints, we sought to investigate this unusual transformation under ball-milling conditions. In this work, we discovered a remarkable reaction pattern, where three distinct pathways are

School of Physical Science and Technology, ShanghaiTech University, 201210 Shanghai, China. E-mail: yankk@shanghaitech.edu.cn

† H. L., Z.-Y. H. and Y.-N. L. contributed equally to this work.

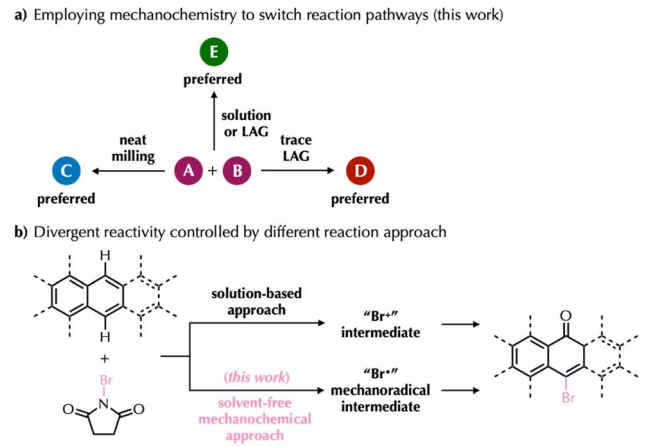

Fig. 1 (a) Divergent reaction pathways controlled by different reaction approaches (amount of LAG solvent: neat milling, trace LAG and excess LAG). (b) the chemical example described in this work.

operative and tunable through ball-milling techniques (Fig. 1a). Explicitly, solvent-free milling favors C–H bromination, while LAG can bias the outcome toward either a selective deformylative bromination (with a trace LAG additive) or an oxidation pathway (with an excess LAG additive) (Fig. 1b). Mechanistic studies indicate that this pathway divergence stems from the generation of different reactive intermediates, dictated by the amount of liquid additive used during ball-milling.

After further screening, we found that the solution reaction between **1a** and **2** in EtOH, in addition to DMF/H_2O, also afforded the oxidation product **3a** (Table 1, entry 13). In contrast, when this reaction was conducted under ball-milling conditions (40 Hz, 1 h) with 2 equiv. of **2**, bromination products were formed selectively (98% combined yield, entry 2). In the product mixture, monobromo- (**3a-Br**) and dibromoanthracene (**3a-Br$_2$**), with the loss of a formyl group, were obtained in 62% and 36% yields, respectively. Only 2% yield of oxidation product **3a-O$_2$** was detected. While other electrophilic brominating agents were investigated, **2** proved the most effective under ball-milling conditions (Table S1). Increasing the milling time to 6 h had little effect on the reaction yields or product distribution (entry 5).[14] Similarly, varying the amount of **2** (1 or 4 equiv.) completely suppressed the oxidation pathway (entries 1 and 3), albeit with diminished bromination efficiency (combined yield of **3a-Br** + **3a-Br$_2$**) (entries 1 and 3). Reaction temperature had a less pronounced impact on the outcome, as the reaction proceeded even at −20 °C (entries 6–7). In contrast, decreasing the milling speed (20 Hz) drastically hampered reactivity (entry 4). This strongly suggests that mechanical impact, rather than the heat generated during the milling process, is a prerequisite for inducing an effective transformation.

These divergent results prompted us to consider whether **3a-Br** serves as an intermediate in the formation of either **3a-Br$_2$** or **3a-O$_2$**. To test this hypothesis, a purified sample of **3a-Br** was subjected to neat milling conditions identical to those in entry 2. However, no further reaction was observed. Similarly, control experiments starting from either **3a-Br$_2$** or **3a-O$_2$** also showed no conversion under these conditions (Fig. 2a). To further

Table 1 Condition screening in the mechanochemical reaction between **1a** and **2** under neat milling[a]

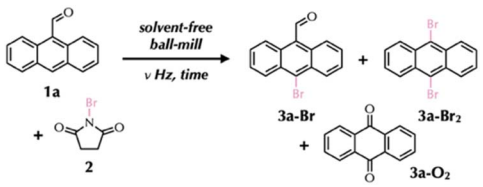

Entry	ν (Hz)	Time (h)	Equiv. of 2	EtOH additive (mL mg^{-1})	Yield (%) of **3a-Br**/**3a-Br$_2$**/**3a-O$_2$**[b]
1	40	1	4	0	59/30/0
2	**40**	**1**	**2**	**0**	**62/36/2**
3	40	1	1	0	52/23/0
4	20	1	2	0	31/12/0
5	40	6	2	0	41/48/5
6	40	1[c]	2	0	67/30/0
7	40	1[c]	2	0	42/20/0
8	**40**	**1**	**2**	**0.1**	**19/71/trace**
9	40	1	2	0.2	20/59/13
10	40	1	2	0.5	3/21/36
11	**40**	**1**	**2**	**2.0**	**3/10/60**
12	40	1	2	4.0	0/2/41
13	—	6	2	Neat	—/—/90[d](75)[e]

[a] Ball milling parameters: 2 mL PP tube and ZrO_2 balls (3.0 mm × 3) under open air condition. [b] Yields and product ratios determined by ^{1}H NMR spectroscopy with hexamethylbenzene as an internal standard. [c] Milling conducted at jar temperatures of 80 °C and −20 °C. [d] Solution reactions conducted in the EtOH solution reaction at 80 °C. [e] or at rt.

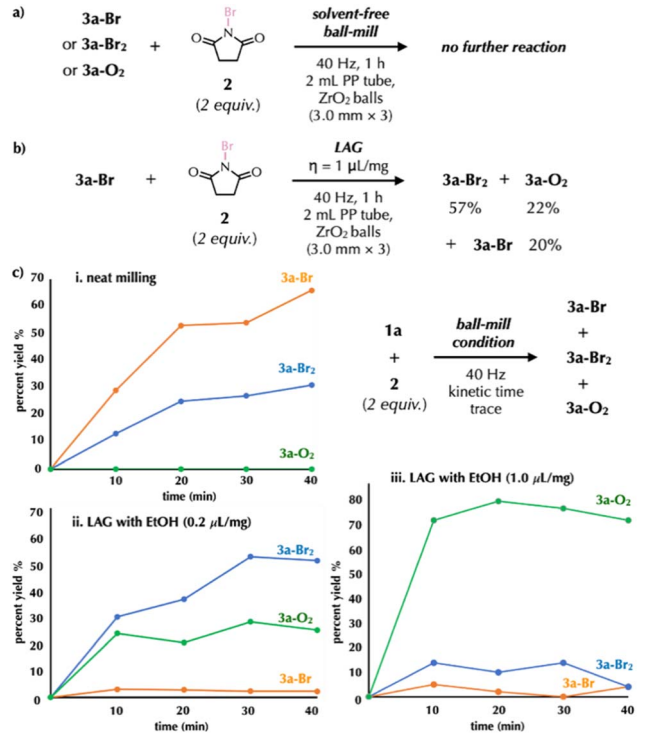

Fig. 2 (a) Control experiments of (a) solvent-free reactions between **3a-Br**, **3a-Br$_2$** and **3a-O$_2$** and **2** and (b) a trace LAG reaction between **3a-Br** and **2**. (c) Reaction progress between **1a** and **2** under different milling conditions: (i) solventless; and LAG with EtOH, (ii) 0.2 μL mg^{-1} and (iii) 1.0 μL mg^{-1}.

elucidate the reaction pathway, we performed kinetic profiling to monitor the product distribution over time (Fig. 2c(i)).[15] These experiments revealed that the ratios of **3a-Br**/**3a-Br$_2$** remained constant throughout the course of reaction, fluctuating only slightly between 2.1 and 2.3 (Fig. 2c).

Based on the observed divergent reactivity between solvent-free milling (**3a-Br** and **3a-Br$_2$**) and solution processes (**3a-O$_2$**), the solvent effect was inspected in the context of LAG. To this end, each sample was injected with a trace amount (0.2 μL mg^{-1}) of a common organic solvent prior to milling treatment. Regardless of dielectric constant or proticity of the solvents used, these reactions predominantly favored bromination products (Table S2). Among them, only alcoholic solvents such as EtOH bias the formation of **3a-Br$_2$**, up to 19 : 71 ratio for **3a-Br** and **3a-Br$_2$** (Table 1, entries 8–9). With increasing EtOH additive content, the formation of **3a-O$_2$** increased up to 60% (entries 10–11). Up to 4.0 μL mg^{-1}, the bromination pathway is completely shut down, obeying a thermal reaction pattern in solution (entries 12–13). The kinetic traces (0.2 μL mg^{-1} and 1.0 μL mg^{-1}) also revealed that the major product under each LAG condition (0.2 μL mg^{-1}: **3a-Br$_2$**; 1.0 μL mg^{-1}: **3a-O$_2$**) evolved rapidly and the product ratio was maintained for the rest of reactions (Fig. 2c(ii) and (iii)). In addition, **3a-Br$_2$** only minimally converts to **3a-O$_2$** under LAG conditions (1.0 μL mg^{-1}; 3% yield), while **3a-O$_2$** was completely recovered in an analogous reaction with **2** (2 equiv.). Meanwhile, an isolated sample of **3a-Br** converts to **3a-Br$_2$** and **3a-O$_2$** in 57% and 22% yields under LAG conditions (1.0 μL mg^{-1}), respectively (Fig. 2b). This information suggests that three reactions between **1a** and **2** proceed under kinetic control driven by the amount of solvent employed (solvent-free mechanochemical *vs.* LAG *vs.* solution-phase methods).

We next turned our attention to mechanistic understanding in the bromination reaction with **2** in ball-milling methods. When a spin-trapping agent, such as TEMPO, BHT or allyl-(2,2,6,6-tetramethylpiperidin-1-yl)oxyl (TEMPO)-based radical trap CHANT[16] (2 equiv.), was added to a neat milling reaction between **1a** and **2**, the reactions were inhibited and **1a** was fully recovered (Fig. 3a(i)). In the reaction with CHANT, the ESI-MS spectrum revealed the formation of new adducts **4** (calc. [M +

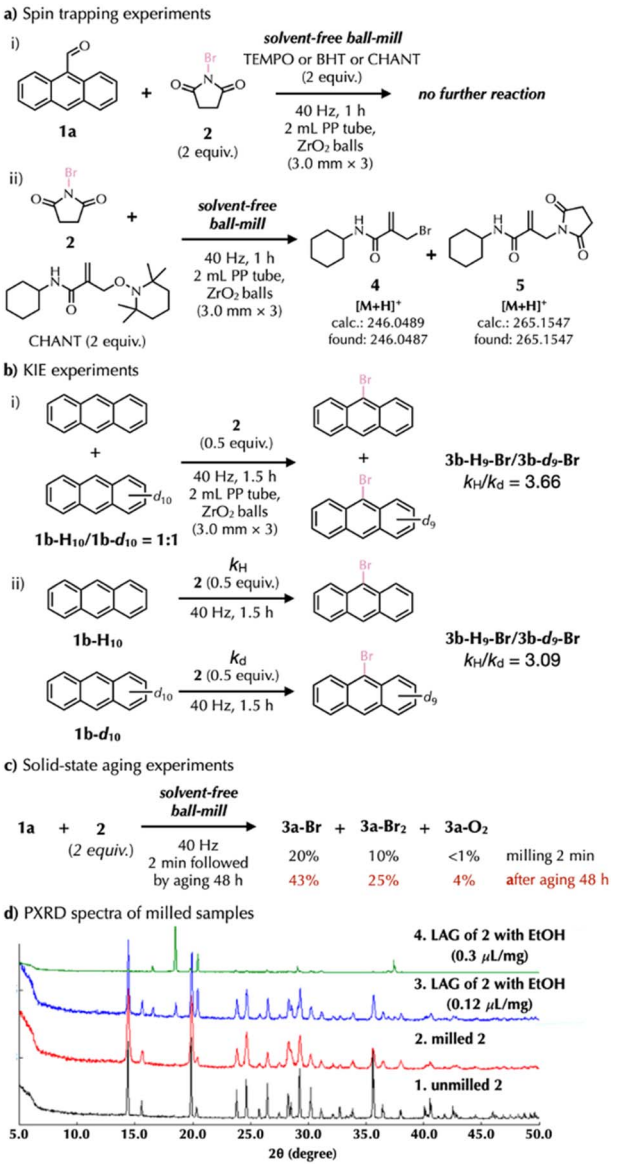

Fig. 3 Mechanistic studies with (a) spin-trapping reagents; and (b) KIE experiments determined (i) from an intermolecular competition and (ii) from two parallel reactions. (c) Solid-state aging experiments; and (d) PXRD experiments of **2** under different milling treatments.

$H]^+$ 264.0489; found 264.0487) and **5** (calc. $[M + H]^+$ 265.1547; found 265.1547) (Fig. 3a(ii)), derived from Br$^\bullet$ or succinimide radical olefin addition in CHANT, respectively. The radical nature of the bromination reaction with **2** is further supported by the negative attempt with 5,5-dibromo-2,2-dimethyl-1,3-dioxane-4,6-dione (**2-ii**), as an alternative brominating agent in the reaction with **1a**, where cleaving the C–Br bond is unlikely (Table S1). Moreover, KIE experiments with anthracene (**1b-H$_{10}$**/**1b-*d*$_{10}$**) gave k_H/k_D values of 3.09–3.66, supporting C–H bond cleavage as the rate determining step (Fig. 3b). Considering the solid-state packing effect, a milling reaction (40 Hz) between **1a** and **2** was intentionally paused after 2 min. Storing or "aging" the milled sample in the dark for 48 h facilitated the conversion of **3a-Br** and **3a-Br$_2$** from 20% and 10% (immediately after ball-milling) to 43% and 25% yield, respectively (Fig. 3c).[17,18] These experiments suggest that bromination with **2** likely follows a radical pathway, and the initiation occurring through homolysis of the N–Br bond of **2** *via* mechanical impact generated from a ball-milling process. Once mechanoradicals (Br$^\bullet$ or succinimide radicals) are formed and stabilized within solid-state packing (see PXRD discussion below), as evident from the aging experiments, bromination could follow a chain-like mechanism even in the absence of mechanical impact, suggested by the aging experiments.

To identify the active brominating species in LAG and solution-based processes, we analyzed the reaction mixture. When **2** was milled with a trace amount of EtOH (under LAG conditions), the ^{1}H NMR spectrum of the milled sample (**6**) in $CDCl_3$ revealed a new set of ethyl C–H resonances ~0.5 ppm more downfield shifted than those in free EtOH, indicating the formation of a more electrophilic species (Fig. S8). This unexpected species **6** was tentatively assigned as $[EtOHBr]^+$, structurally analogous to other active species responsible for electrophilic bromination formed *in situ* from Lewis bases and **2**.[19] We propose that highly reactive intermediates, such as bromine radicals (Br$^\bullet$) in solvent-free milling and complex **6** ("Br$^+$") in LAG, are stabilized by the confinement effect within the crystalline phases. This hypothesis is supported by PXRD studies (Fig. 3d), which showed well-defined diffraction patterns for both neat milling (pure crystal phase of **2** in Fig. 3d(2)) and trace LAG samples (pure crystal phase of succinimide (**7**) in Fig. 3d(4)), indicating the existence of a crystalline environment. In the absence of the crystalline lattice, species **6** can neither be isolated nor detected under conventional solution-based reaction conditions (Table 1, entry 13), consistent with the absence of such a stabilizing solid-state confinement effect.

The origin of oxygen atoms in **3a-O$_2$** represents the final piece of the mechanistic puzzle. To identify this source, we conducted the following experiments. First, the reaction of **1a** with succinimide (**7**) under standard conditions did not produce **3a-O$_2$**, ruling out **2** as the oxygen source. Second, LAG reactions of **1a** and **2** with EtOH under a N_2 atmosphere still gave **3a-O$_2$**. Third, and conclusively, an LAG reaction employing $H_2{}^{18}O$ (η = 1.0) furnished **3a-^{18}O$_2$**, as confirmed by HRMS analysis (calc. for $[M + H]^+$ 213.0682; found 213.0682) (Fig. S5). In addition, reactions under anhydrous ethanol still produced

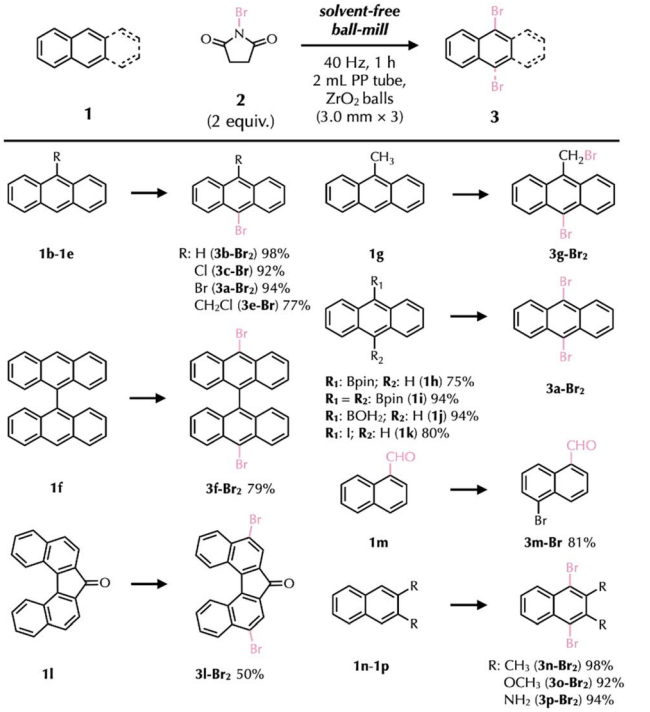

Fig. 4 Substrate scope in the mechanochemical reaction between **1** and **2** under solvent-free conditions. Yields determined by ^{1}H NMR spectroscopy with an internal standard. The experimental details for the isolation procedure and isolated yields for some of the products are described in the SI.

3a-O$_2$, and these results confirm that protic solvents, including alcohols and water, can both serve as the source of oxygen atoms **in 3a-O$_2$**.

To evaluate the synthetic utility of solvent-free mechanochemical bromination, various naphthalene and anthracene derivatives were treated with **2** (2 equiv.) at 40 Hz for 1 h (Fig. 4). Substrates including anthracene (**1b**), 9-chloroanthracene (**1c**), 9-bromoanthracene (**1d**), 9-(chloromethyl)anthracene (**1e**), and 9,9′- bianthracene (**1f**) were efficiently converted to their corresponding dibrominated products (**3b-Br$_2$** to **3f-Br$_2$**). In contrast, anthracene derivatives bearing -Bpin (**1h**), -(Bpin)$_2$ (**1i**), -B(OH)$_2$ (**1j**), and -I (**1k**) underwent a tandem defunctionalization and dibromination, yielding **3-Br$_2$** as the sole product. The reaction of 9-methylanthracene (**1g**) with **2** resulted in sp^3-CH bromination (**3g-Br$_2$**) in 44% yield, a result that supports a radical-mediated mechanism. Naphthalene derivatives containing either electron-withdrawing (**1m**) or electron-donating groups (**1n–1p**) were well tolerated, affording **3m-Br** to **3p-Br$_2$** in good yields. Notably, the solution-phase reaction of **1m** with **2** led to the formation of 1,4-naphthoquinone, mirroring the divergent reactivity observed for **1a** and highlighting a key distinction from the mechanochemical process.[13] Finally, 7*H*-dibenzo[*c*,*g*]fluoren-7-one (**1l**), a twisted aryl ketone and key precursor for organic semiconductors,[20] persistent organic radicals,[21] and Feringa-type molecular rotors,[22] was successfully dibrominated under the standard conditions, yielding **3l-Br$_2$** in 50% yield.

Conclusions

In summary, we have developed a mechanochemical strategy that selectively biases reaction pathways toward either C–H bromination or oxidation. Mechanistic investigations indicate that the mechanochemical environment favors a radical-chain pathway for C–H bromination, whereas solution conditions promote oxidation *via* brominium-like intermediates. Crucially, this work demonstrates that mechanochemistry can stabilize reactive species and thereby unlock distinct chemical space with reactivity divergent from that observed in solution. This ability to access hidden reagent reactivity underscores the potential of mechanochemistry to complement and expand the toolbox of conventional synthetic methods.

Author contributions

The work was conceptualized by H. L. and K. Y. All experiments were conducted by H. L, Z. H, Y. L, Y. J. and T. W. The manuscript was written by K. Y. with the input from all the authors. All authors have given approval to the final version of the manuscript.

Conflicts of interest

There are no conflicts to declare.

Data availability

The data supporting this article have been included as part of the supplementary information (SI). Supplementary information is available. See DOI: https://doi.org/10.1039/d5mr00104h.

Acknowledgements

Financial support for this work was generously provided by the ShanghaiTech University start-up funding. We also thank other staff members at the Analytical Instrumentation Center of SPST, and ShanghaiTech University (contract no. SPST-AIC10112914) for characterization support.

Notes and references

1 (*a*) S. L. James, C. J. Adams, C. Bolm, D. Braga, P. Collier, T. Friščić, F. Grepioni, K. D. Harris, G. Hyett, W. Jones, A. Krebs, J. Mack, L. Maini, A. G. Orpen, I. P. Parkin, W. C. Shearouse, J. W. Steed and D. C. Waddell, *Chem. Soc. Rev.*, 2012, **41**, 413–447; (*b*) K. J. Ardila-Fierro and J. G. Hernandez, *ChemSusChem*, 2021, **14**, 2145–2162; (*c*) E. Colacino, V. Isoni, D. Crawford and F. García, *Trends Chem.*, 2021, **3**, 335–339; (*d*) J. L. Howard, Q. Cao and D. L. Browne, *Chem. Sci.*, 2018, **9**, 3080–3094; (*e*) D. Virieux, F. Delogu, A. Porcheddu, F. García and E. Colacino, *J. Org. Chem.*, 2021, **86**, 13885–13894; (*f*) F. León and F. García, in *Comprehensive Coordination Chemistry III*, ed. E. C. Constable, G. Parkin and L. Que Jr, 3rd edn, 2021; (*g*) R. Liu, X. He, T. Liu, X. Wang, Q. Wang, X. Chen and Z. Lian, *Chem.–Eur. J.*, 2024, **30**, e202401376.

2 (*a*) C. Bolm and J. G. Hernandez, *Angew. Chem., Int. Ed.*, 2019, **58**, 3285–3299; (*b*) K. Y. Jia, J. B. Yu, Z. J. Jiang and W. K. Su, *J. Org. Chem.*, 2016, **81**, 6049–6055; (*c*) Y. Liu, F. Z. Liu and K. Yan, *Angew. Chem., Int. Ed.*, 2022, **61**, e202116980; (*d*) N. Haruta, T. Sato and K. Tanaka, *Tetrahedron Lett.*, 2013, **54**, 5290–5293; (*e*) J.-L. Do and T. Friščić, *ACS Cent. Sci.*, 2017, **3**, 13–19; (*f*) J. G. Hernández and C. Bolm, *J. Org. Chem.*, 2017, **82**, 4007–4019; (*g*) F. Cuccu, L. De Luca, F. Delogu, E. Colacino, N. Solin, R. Mocci and A. Porcheddu, *ChemSusChem*, 2022, **15**, e202200362.

3 T. Seo, K. Kubota and H. Ito, *Angew. Chem., Int. Ed.*, 2020, **58**, 3285–3299.

4 J. L. Howard, M. C. Brand and D. L. Browne, *Angew. Chem., Int. Ed.*, 2018, **57**, 16104–16108.

5 S. Kaabel, R. S. Stein, M. Fomitsenko, I. Jarving, T. Friščić and R. Aav, *Angew. Chem., Int. Ed.*, 2019, **58**, 6230–6234.

6 L. Chen, M. Regan and J. Mack, *ACS Catal.*, 2016, **6**, 868–872.

7 (*a*) I. Saikia, A. J. Borah and P. Phukan, *Chem. Rev.*, 2016, **116**, 6837–7042; (*b*) D. A. Petrone, J. Ye and M. Lautens, *Chem. Rev.*, 2016, **116**, 8003–8104.

8 (*a*) A. Krasovskiy, A. Tishkov, V. Del Amo, H. Mayr and P. Knochel, *Angew. Chem., Int. Ed.*, 2006, **45**, 5010–5014; (*b*) T. Nagano and T. Hayashi, *Org. Lett.*, 2005, **7**, 491–493; (*c*) For their mechanochemical analogues, see ref. 9d–f; (*d*) R. Takahashi, A. Hu, P. Gao, Y. Gao, Y. Pang, T. Seo, J. Jiang, S. Maeda, H. Takaya, K. Kubota and H. Ito, *Nat. Commun.*, 2021, **12**, 6691; (*e*) P. Gao, J. Jiang, S. Maeda, K. Kubota and H. Ito, *Angew. Chem., Int. Ed.*, 2022, **61**, e202207118.

9 (*a*) *Metal-Catalyzed Cross-Coupling Reactions*, ed. A. de Meijere and F. Diederich, Wiley-VCH, Germany, 2nd edn, 2024; (*b*) For mechanochemical analogues, see ref. 9c and d; (*c*) K. Kubota and H. Ito, *Trends Chem.*, 2020, **2**, 1066–1081; (*d*) C. Wu, J. Lv, H. Fan, W. Su, X. Cai and J. Yu, *Chem.–Eur. J.*, 2024, **30**, e202304231.

10 (*a*) C. K. Prier, D. A. Rankic and D. W. MacMillan, *Chem. Rev.*, 2013, **113**, 5322–5363; (*b*) K. Kubota, Y. Pang, A. Miura and H. Ito, *Science*, 2019, **366**, 1500–1504; (*c*) C. Schumacher, J. G. Hernandez and C. Bolm, *Angew. Chem., Int. Ed.*, 2020, **59**, 16357–16360.

11 (*a*) D. Margetič and V. Štrukil, *Mechanochemical Organic Synthesis*, Elsevier: Boston, 2016, pp. 235–282; (*b*) N. N. Karade, G. B. Tiwari, D. B. Huple and T. A. J. Siddiqui, *J. Chem. Res.*, 2006, 366–368; (*c*) A. Bose and P. Mal, *Tetrahedron Lett.*, 2014, **55**, 2154–2156; (*d*) S. K. Bera and P. Mal, *J. Org. Chem.*, 2021, **86**, 14144–14159; (*e*) A. Bal, T. Kumar Dinda and P. Mal, *Asian J. Org. Chem.*, 2022, **11**, e202200046; (*f*) K. J. Ardila-Fierro, L. Vugrin, I. Halasz, A. Palčić and J. G. Hernández, *Chem.:Methods*, 2022, **2**, e202200035; (*g*) G.-W. Wang and J. Gao, *Green Chem.*, 2012, **14**, 1125–1131; (*h*) Z. Liu, H. Xu and G. W. Wang, *Beilstein J. Org. Chem.*, 2018, **14**, 430–435; (*i*) D. Barišić, I. Halasz, A. Bjelopetrović, D. Babić and M. Ćurić, *Organometallics*, 2022, **41**, 1284–1294; (*j*) J. Wong and Y. Y. Yeung, *RSC Adv.*, 2021, **11**, 13564–13570; (*k*)

S. Patra, V. Valsamidou, B. N. Nandasana and D. Katayev, *ACS Catal.*, 2024, **14**, 13747–13758; (*l*) S. Patra, B. N. Nandasana, V. Valsamidou and D. Katayev, *Adv. Sci.*, 2024, **11**, e2402970; (*m*) D. Das, A. A. Bhosle, A. Chatterjee and M. Banerjee, *Beilstein J. Org. Chem.*, 2022, **18**, 999–1008; (*n*) E. Bartalucci, C. Schumacher, L. Hendrickx, F. Puccetti, I. d'Anciães Almeida Silva, R. Dervişoğlu, R. Puttreddy, C. Bolm and T. Wiegand, *Chem.–Eur. J.*, 2023, **29**, e202203466; (*o*) D. Barišić, M. Pajić, I. Halasz, D. Babić and M. Ćurić, *Beilstein J. Org. Chem.*, 2022, **18**, 680–687.

12 H. Luo, F. Z. Liu, Y. Liu, Z. Chu and K. Yan, *J. Am. Chem. Soc.*, 2023, **145**, 15118–15127.

13 P. Natarajan, V. D. Vagicherla and M. T. Vijayan, *Tetrahedron Lett.*, 2014, **55**, 3511–3515.

14 The conflicting data in Table 1 (entries 1 *vs.* 5), where longer milling times between **1a** and **2** lead to the conversion of **3a-Br** to **3a-Br$_2$** and **3a-O$_2$**, but not in the reaction shown in Fig. 2a, were further investigated. It was revealed that the conversion of **3a-Br** to **3a-Br$_2$** under neat milling becomes evident upon extended grinding (up to 3 h), as shown in Fig. 2c and Table S7. This supports a stepwise bromination mechanism: (i) initial phase (0–1 h): competitive formation of **3a-Br** and **3a-Br$_2$** *via* parallel radical pathways (competitive C–H abstraction by Br$^{\bullet}$). (ii) Later phase (1–6 h): gradual and slow secondary bromination of **3a-Br** by residual **2**, driven by persistent mechanical activation. Control experiments with isolated **3a-Br** confirmed its conversion to **3a-Br2** (6% after 3 h) only in the presence of fresh **2**.

15 As each time point requires pausing the ball-milling reaction and removing samples from the reaction vessel for periodic NMR analysis, each data point was obtained from an individual experiment.

16 P. J. H. Williams, G. A. Boustead, D. E. Heard, P. W. Seakins, A. R. Rickard and V. Chechik, *J. Am. Chem. Soc.*, 2022, **144**, 15969–15976.

17 Similar packing-induced reactivity in the solid state was previously observed and reported in ref. 17.

18 W. Ma, Y. Liu, N. Yu and K. Yan, *ACS Sustainable Chem. Eng.*, 2021, **9**, 16092–16102.

19 P. H. Huy, *Eur. J. Org Chem.*, 2020, 10–27.

20 T. Nematiaram, D. Padula, A. Landi and A. Troisi, *Adv. Funct. Mater.*, 2020, **30**, 2001906.

21 Y. Tian, K. Uchida, H. Kurata, Y. Hirao, T. Nishiuchi and T. Kubo, *J. Am. Chem. Soc.*, 2014, **136**, 12784–12793.

22 T. van Leeuwen, J. Pol, D. Roke, S. J. Wezenberg and B. L. Feringa, *Org. Lett.*, 2017, **19**, 1402–1405.